Structural and functional mimic of galactose oxidase by a copper complex of a sterically demanding [N_2O_2] ligand†

Alex John,[a] Mobin M. Shaikh[b] and Prasenjit Ghosh*[a]

Received 28th January 2008, Accepted 13th March 2008
First published as an Advance Article on the web 18th April 2008
DOI: 10.1039/b801496e

A structural and functional mimic of the galactose oxidase (GOase) enzyme active-site by a copper complex supported over a sterically demanding ligand having [N_2O_2] donor sites is reported. Specifically, the binding of the histidine (496 and 581) and tyrosine (272 and 495) residues to the copper center in a square-pyramidal fashion in the active-site of galactose oxidase (GOase) enzyme has been modeled in a copper complex, {[(3-*tert*-butyl-5-methyl-2-hydoxybenzyl)(3′-*tert*-butyl-5′-methyl-2′-oxobenzyl)(2-pyridylmethyl)]amine}Cu(OAc)} (**1b**), stabilized over a sterically demanding ligand in which the two phenolate-*O* atoms mimicked the tyrosine binding while an amine-*N* and pyridyl-*N* atoms emulated the histidine binding to the metal center, similar to that in the enzyme active-site. Furthermore, the copper complex **1b** is found to be an effective functional model of the enzyme as it efficiently catalyzed the chemoselective oxidation of primary alcohols to aldehydes in high turnover numbers under ambient conditions. An insight into the nature of the active-species was obtained by EPR and CV studies, which in conjunction with the DFT studies, revealed that the active-species is an anti-ferromagnetically coupled diamagnetic radical cation, ^{1}**1b**$^+$, obtained by one electron oxidation at the equatorial phenolate-*O* atom of the ligand in the **1b** complex.

Introduction

Galactose oxidase (GOase) is an important mononuclear Type II copper fungal enzyme that effectively carries out conversion of primary alcohols to aldehydes under ambient aerobic conditions.[1] The tertiary structure of the 68 kDa GOase enzyme exhibits three domains (D1, D2 and D3) comprising of 43 β-strands and one small α-helix built from a single polypeptide chain of 639 amino acid residues. The active-site of the GOase consists of a distorted square-pyramidal copper(II) center coordinated to two histidine (496 and 581), and two tyrosine (272 and 495) residues of the protein backbone along with an exogenous water (at pH = 7) or an acetate (pH = 4.5) moiety and is located on the surface of domain D2 in a hydrophobic region rich with aromatic residues.[2,3] The enzyme efficiently uses molecular oxygen in air in achieving a *two-electron* oxidation of a wide variety of primary alcohol substrates to aldehydes[4] *via* a rare concerted redox cooperativity pathway existing between a neighboring radical cofactor, a tyrosine (272) residue, and the redox active copper(II/I) metal center in the enzyme active-site.[5,6] Worth noting that the radical cofactor, tyrosine (272), which undergoes the rare tyrosyl/tyrosinate redox shuttle, is uniquely bound to a nearby cysteine (228) residue through a covalent thioether linkage.[7] Interestingly, the active form of the enzyme is an anti-ferromagnetically coupled diamagnetic species that is EPR silent and which results from the coupling of the radical cofactor, the tyrosine (272) residue, with the metal based unpaired electron of the copper(II) center in the active-site.[8]

A formidable challenge in designing synthetic models of GOase, especially the functional ones, therefore lies in mimicking this tyrosyl/tyrosinate and the Cu(II)/Cu(I) redox couple in small molecule copper complexes. Furthermore, as the catalytic reactivity of the synthetic model is largely dependent on the organic radical–Cu(II/I) redox couple, the proper control of the organic radical center in a model complex, particularly with respect to its stability, magnetic properties and reactivity, are of prime importance. The strategies often employed in fine-tuning the organic radical reactivity thus involve varying several mutually dependent factors like, the state of the phenol moiety (protonated *vs.* deprotonated), the geometrical arrangement around the metal center (axial or equatorial) and the electronic properties of the ligand stabilizing the synthetic model.[9] Towards this end, several ligand systems having N_2O_2 and N_3O donor sets have been extensively used in the GOase biomimetic modeling studies.[9,10] Of special mention are the tripodal N_2O_2 ligands with a pyridyl-*N*, a tertiary amine-*N*, and two phenolate-*O* donor atoms, which successfully emulated the radical cofactor-Cu(II/I) redox couple in its synthetic model complexes and did so specifically by selective deprotonation of the equatorial phenolate-*O*, which transforms to a radical cofactor upon oxidation during the catalysis, while the axial phenolate-*O* remains protonated in these model complexes. This selective deprotonation of the equatorial phenolate-*O* has not only been achieved by distinguishing the two phenolate-*O* moieties by incorporating different substituents on the respective phenyl rings, as

[a]*Department of Chemistry, Indian Institute of Technology Bombay, Powai, Mumbai, 400 076, India. E-mail: pghosh@chem.iitb.ac.in; Fax: +91-22-2572-3480; Tel: +91-22-2576-7178*
[b]*National Single Crystal X-ray Diffraction Facility, Indian Institute of Technology Bombay, Powai, Mumbai, 400 076, India*

† Electronic supplementary information (ESI) available: X-Ray metrical data comparison table, the B3LYP coordinates of the optimized geometries for ^{2}**1b**, ^{3}**1b**$^+$, ^{4}**1b**$^{2+}$, intermediate **1**, intermediate **2** and intermediate **3** along with the comparison tables, spin density table, frontier molecular orbital diagrams, cyclic voltammogram and electronic spectroscopic data. CCDC reference number 640145. For ESI and crystallographic data in CIF or other electronic format see DOI: 10.1039/b801496e

in the {[(3-*tert*-butyl-5-methoxy-2-hydoxybenzyl)(3′-*tert*-butyl-5′-nitro-2′-oxobenzyl)(2-pyridylmethyl)]amine}Cu(OAc) complex,[11] but also in a case where they are the same as observed in the {[(3,5-di-*tert*-butyl-2-hydoxybenzyl)(3′,5′-di-*tert*-butyl-2′-oxobenzyl)(2-pyridylmethyl)]amine}Cu(OAc) complex.[12] Because of the aforementioned reasons, we decided to employ a new sterically demanding variant of the N_2O_2 tripodal ligand, bis(3-*tert*-butyl-5-methyl-2-hydroxybenzyl)(2-pyridylmethyl)amine (**1a**) for the purpose of our enzyme biomimetic studies. Furthermore, we rationalized, particularly keeping the functional model of GOase in mind, that the coupling of a stable ligand-based redox center with an adjacent redox active and coordinatively unsaturated Cu(II)/Cu(I) site in the copper complexes would result in generation of novel catalysts capable of oxidation reactions.

Here in this contribution, we report a mononuclear copper complex supported over a tripodal N_2O_2 ligand that not only structurally resembles the active-site of GOase, but also functionally mimics the enzyme activity in carrying out *two-electron* oxidation of a wide variety of primary alcohol substrates to the corresponding aldehydes under ambient conditions, employing a not so common organic radical–Cu(II/I) coupled redox pathway similar to what is observed in the active enzyme.

Results and discussion

The primary challenge in the biomimetic studies of GOase had been in emulating the entire structural, spectroscopic and the functional aspects of the enzyme in totality in small molecule synthetic analogs. As a consequence, despite enormous body of literature[13,14] that exist on the modeling studies of GOase, the examples of metal complexes that simultaneously serve as both the structural and the functional model of the enzyme, particularly with respect to mimicking the unconventional radical cofactor-Cu(II/I) redox coupled pathway as seen in the enzyme, are strikingly few in number. For example, the representative examples of a few copper complexes that would genuinely qualify as both the structural and functional model of GOase are stabilized over N_2O_2 ligands.[10h,11,15–17] Interestingly enough, while the {[(3-*tert*-butyl-5-methoxy-2-hydoxybenzyl)(3′-*tert*-butyl-5′-nitro-2′-oxobenzyl)(2-pyridylmethyl)]amine}Cu(OAc) complex,[11] which is supported over a tripodal N_2O_2 ligand with two different phenolate-O sidearms serves as an excellent structural and functional model of GOase, a related analog, {[(3,5-di-*tert*-butyl-2-hydoxybenzyl)(3′,5′-di-*tert*-butyl-2′-oxobenzyl)(2-pyridylmethyl)]amine}Cu(OAc),[12] stabilized over another variant of the same N_2O_2 ligand but having same phenolate-*O* sidearms serves only as a structural model and does not exhibit any biomimetic functional attributes. Hence, we became interested in designing a structural and functional model of a N_2O_2 ligand, bis(3-*tert*-butyl-5-methyl-2-hydroxybenzyl)(2-pyridylmethyl)amine (**1a**), possessing two same phenolate-*O* sidearms by fine-tuning its steric and electronic properties.

In this regard, the tripodal ligand **1a** was synthesized by a Mannich condensation reaction of 2-*tert*-butyl-4-methylphenol with 2-(aminomethyl)pyridine in 55% yield while the corresponding copper complex, {[(3-*tert*-butyl-5-methyl-2-hydoxybenzyl)(3′-*tert*-butyl-5′-methyl-2′-oxobenzyl)(2-pyridylmethyl)]amine}Cu(OAc) **1b**, was obtained by the treatment of the ligand **1a** with $Cu(OAc)_2{\cdot}H_2O$ in methanol in 43% yield (Scheme 1) and the paramagnetic complex was characterized by IR, electronic spectroscopy, EPR, elemental analysis and X-ray diffraction studies.

The most remarkable feature of the **1b** complex is its similarity with the GOase active-site (Fig. 1 and 2). Specifically, the Cu center in **1b** was found to bind with two O donors, mimicking the tyrosine (Tyr 272 and Tyr 495) binding, and to two N donors, also emulating the histidine (His 581 and His 496) binding, in a square pyramidal fashion similar to that seen in the enzyme active-site (Table S1, ESI†). The equatorial square plane around the central Cu^{2+} in **1b** was thus formed by two N atoms (amine *N* and the pyridine *N*), two O atoms (phenolate *O* and acetate *O*) while the non-deprotonated phenol (phenyl-*OH*) was found to bind to the metal from the axial position. Apart from the direct correlation with the enzyme active-site, the copper complex **1b** was also found to be in good agreement with two other structurally similar GOase model complexes (Table S1, ESI†).[11,12] In this regard, worth mentioning that the square pyramidal geometry around the Cu(II) center in the active-site of GOase is vital to its function as it orients the methylene hydrogen of the substrate alcohol in close vicinity of the tyrosyl radical in the active enzyme to facilitate

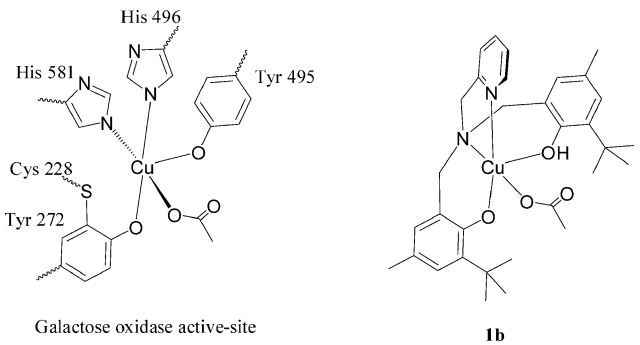

Fig. 1

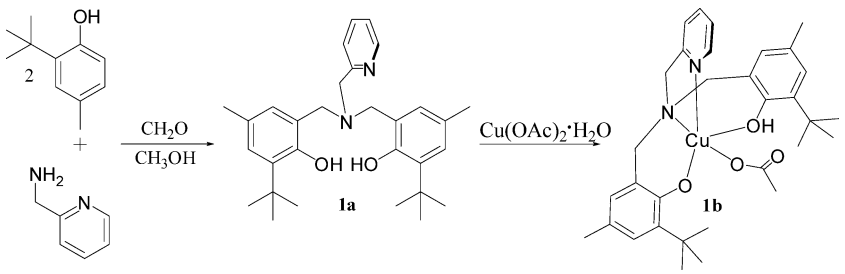

Scheme 1

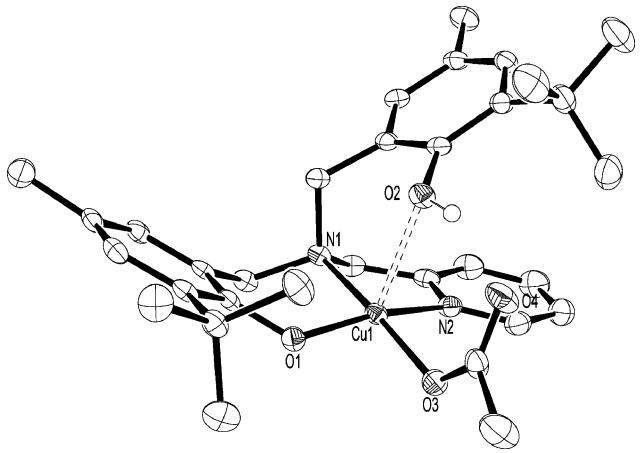

Fig. 2 ORTEP of **1b**. Selected bond lengths (Å) and angles (°): Cu1–O1 1.8871(14), Cu1–O3 1.9582 (15), Cu1–N1 2.0340(18), Cu1–N2 1.9967(18), O2–H102 0.75(3); O1–Cu1–O3 87.19(6), O1–Cu1–N2 166.86(7), O3–Cu1–N2 93.58(7), O1–Cu1–N1 94.12(7), O3–Cu1–N1 174.01(7).

the hydrogen atom transfer (HAT) process. Given the observation that the coordination environment around **1b** closely resembles the active-site geometry of GOase, the copper complex is expected to emulate the functional activity of the enzyme.[6c,18]

In order to obtain insight on the electronic structure of the copper complex **1b**, density functional theory studies were carried out and the geometry optimized structure of the complex **1b** was computed at the B3LYP/LANL2DZ, 6–31G(d) level of theory using the atomic coordinates adopted from X-ray analysis and subsequently, single-point calculation was performed at the same level of theory for detailed prediction of the electronic properties of the complex. The optimized structure of ^{2}**1b** (Fig. S1, ESI†) exhibited a square pyramidal geometry around the central Cu^{2+} ion with the protonated phenol moiety occupying the axial position in a manner similar to that observed in the X-ray structure. Inspection of the frontier molecular orbitals of the optimized structure reveals an arrangement characteristic of square-pyramidal copper complexes with an one electron vacancy in the 150β orbital localized on the Cu $d_{x^2-y^2}$ orbital. In general, the optimized bond lengths are in good agreement with those of the crystallographic data (Table S8, ESI†).

As the enzyme is known to exist in three well defined oxidation levels, (i) an EPR silent active form (cupric ion antiferromagnetically coupled to the equatorial phenoxy radical), (ii) an intermediate form and (iii) the reduced Cu(I) form (Scheme 2), we became interested in investigating the relevance of these species particularly with respect to the functioning of our GOase model **1b** complex. In particular, with the aim of exploring the feasibility of the unconventional radical cofactor–Cu(II/I) redox coupled pathway occurring in the GOase model **1b** complex, we wanted to look into the possibility of the ligand based *one-electron* oxidation occurring on the equatorial phenolate-*O* atom of ^{2}**1b**, thereby generating a organic radical center adjacent to the paramagnetic Cu(II) center in the copper complex, similar to what is seen in the

$$Cu^{II}\text{-}Tyr^{\bullet+} \underset{}{\overset{e^-}{\rightleftharpoons}} Cu^{II}\text{-}Tyr \overset{e^-}{\rightleftharpoons} Cu^{I}\text{-}Tyr$$

Scheme 2

active enzyme, and subsequently yielding an antiferromagnetically coupled diamagnetic species (^{1}**1b**$^+$), instead of the expected lower energy ^{3}**1b**$^+$ species.

Indeed, removal of an electron from the copper complex ^{2}**1b** results in a ligand based oxidation as opposed to the metal based one resulting in the cationic ^{3}**1b**$^+$ species. Inspection of the frontier molecular orbitals of ^{2}**1b** displays a single vacancy in the valence shell 150β (HOMO) located on the Cu $d_{x^2-y^2}$ orbital, which is consistent with a square pyramidal arrangement, while the next lower 149th orbital (HOMO−1) being fully occupied (Fig. S1, ESI†). Thus, the *one-electron* oxidation of ^{2}**1b** yielded the oxidized ^{3}**1b**$^+$ species with two unpaired electrons, one on the Cu $d_{x^2-y^2}$ orbital (150α) as seen from natural bond order (NBO) analysis and the other on the equatorial phenolate ring (149 α) consistent with the adjacent radical cofactor (Tyr 272) and the Cu(II/I) center in the GOase active-site (Fig. 3).

Further support in favor of the *one-electron* ligand-based oxidation comes from the Mulliken spin density analysis (Table S9, ESI†) which revealed that the total spin density (both α and β spins) on the Cu(II) center remains the same [Cu = 0.49 (^{2}**1b**), 0.57 (^{3}**1b**$^+$)] while that on the equatorial phenolate-*O* moiety [0.26 (^{2}**1b**), 1.01 (^{3}**1b**$^+$)] increases drastically upon *one-electron* oxidation of ^{2}**1b** to the ^{3}**1b**$^+$ species.

The clinching evidence in favor of the radical cofactor-Cu(II/I) redox couple existing in the GOase model complex **1b** came from EPR studies, which showed that while the **1b** complex displayed a typical pattern corresponding to one unpaired electron on copper, the electrochemically generated *one-electron* oxidized analog was found to be diamagnetic as a result of antiferromagnetic coupling between the organic radical (equatorial phenolate-*O*) and the adjacent Cu(II) center (Fig. 4). Specifically, the EPR spectrum of **1b** recorded in the frozen state in CH_3CN showed a commonly observed axial pattern with three well resolved peaks in the low field region ($g_\parallel = 2.267$; $A_\parallel = 160$) due to splitting with the Cu nucleus ($I = 3/2$) and a high intensity peak in the high field region ($g_\perp = 2.046$; $A_\perp$ = NR). The observed values are in concurrence with not only the reported values for the inactive form of the enzyme GOase ($g_\parallel = 2.277$; $g_\perp = 2.055$; $A_\parallel = 175$)[19] but also with related GOase synthetic models. For example, the *g* and *A* values reported for a series of structural models of GOase based on bis(pyridyl)alkyl amines are ($g_\parallel = 2.217$–2.327; $g_\perp = 2.04$–2.098 and $A_\parallel = 147$–187) while those exhibited by a series of phenol containing TACN ligand (TACN = 1,4,7-triazacyclononane) lie in the range ($g_\parallel = 2.25$–2.27; $g_\perp = 2.02$–2.06 and $A_\parallel = 157$–175).[13c] Furthermore, the *g* and *A* values exhibited by a related analog namely, {[(3-*tert*-butyl-5-methoxy-2-hydoxybenzyl)(3′-*tert*-butyl-5′-nitro-2′-oxobenzyl)(2-pyridylmethyl)]amine}Cu(OAc), are $g_{xx} = 2.042$; $g_{yy} = 2.059$; $g_{zz} = 2.256$ and $A_{xx} = 1$ mT; $A_{yy} = 2.5$ mT; $A_{zz} = 17.8$ mT, respectively.[11] In addition, the higher value of $g_\parallel$ (2.267) as compared to $g_\perp$ (2.046) in the **1b** complex indicates that the unpaired electron of the Cu(II) center resides on the metal $d_{x^2-y^2}$ orbital as was also confirmed by NBO studies. In this regard it is worth mentioning that for the tetragonal and square planar Cu(II) complexes that exhibit $g_\parallel > g_\perp$ the unpaired electron is reported to reside on the $d_{x^2-y^2}$ orbital.[20]

More importantly, frozen-state EPR measurements carried out on the electrochemically oxidized species of **1b** showed it to be diamagnetic in nature indicating a significant antiferromagnetic coupling occurring between the unpaired $d_{x^2-y^2}$ electron on Cu^{2+}

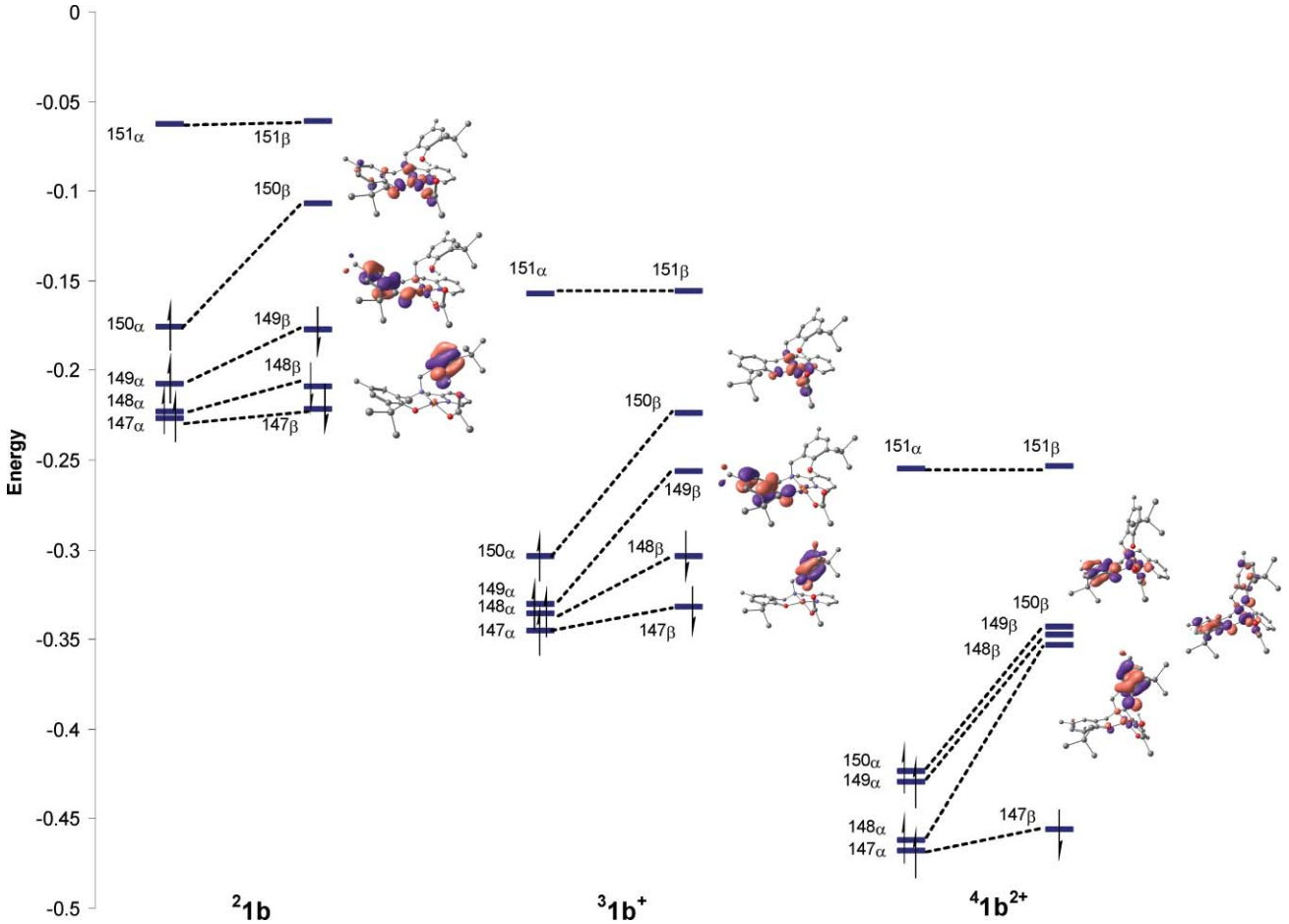

Fig. 3 Frontier molecular orbitals of ^{2}**1b**, ^{3}**1b**$^+$ and ^{4}**1b**$^{2+}$ showing the electronic arrangement; orbitals corresponding to molecular orbital number 150, 149 and 148 are shown (energy is given in Hartrees).

with the phenoxy-radical (suggesting the formation of ^{1}**1b**$^+$ species) similar to the tyrosyl (272) radical–Cu(II) redox couple seen in the active enzyme (Fig. 4).

Further insights on the nature of the oxidized species of the **1b** complex were obtained from the cyclic voltammetry (CV) studies which were in concurrence with the EPR results. Specifically, the cyclic voltammogram (CV) of the copper complex (**1b**) in CH_3CN–CH_2Cl_2 (1 : 1) at room temperature, exhibited two electrochemical processes in the anodic region on the CV timescale, but no processes were observed in the negative region [between 0 and −0.5 V *vs.* Ag/AgCl] (Fig. S2, ESI† and Scheme 3). The first quasi-reversible electrochemical process appeared at $E_{1/2}$ = 0.72 V (ΔE = 82 mV) [$E_{1/2}$ = 0.21 V *vs.* $FeCp_2/FeCp_2^+$] and the second quasi-reversible process at $E_{1/2}$ = 1.10 V (ΔE = 94 mV) [$E_{1/2}$ = 0.60 V *vs.* $FeCp_2/FeCp_2^+$]. Comparison of the electrochemical nature of complex **1b** with related copper bisphenolate complexes confirms that both the oxidation processes ($E_{1/2}$ = 0.21 V and $E_{1/2}$ = 0.60 V; *vs.* $FeCp_2/FeCp_2^+$) arise due to ligand based oxidation of the phenol

$$\underset{^2\mathbf{1b}}{[Cu^{II}(OAc)\text{-}LH]} \overset{-e^-}{\rightleftharpoons} \underset{^1\mathbf{1b}^+}{[Cu^{II}(OAc)\text{-}\overset{\bullet+}{L}H]} \overset{-e^-}{\rightleftharpoons} \underset{^4\mathbf{1b}^{2+}}{[Cu^{II}(OAc)\text{-}\overset{\bullet\bullet}{L}H]}$$

Scheme 3

moiety to phenoxy radicals. For example, the structurally related complex {[(3-*tert*-butyl-5-methoxy-2-hydoxybenzyl)(3′-*tert*-butyl-5′-nitro-2′-oxobenzyl)(2-pyridylmethyl)]amine}Cu(OAc) showed a reversible one-electron oxidation peaks at $E_{1/2}$ = 0.075 V (*vs.* $FeCp_2/FeCp_2^+$) {1 mM in CH_3CN–CH_2Cl_2 (1 : 1), TBAP (100 mM), scan rate 100 mV s^{-1}}[11] and another analogous complex namely, {[(3,5-di-*tert*-butyl-2-hydoxybenzyl)(3′,5′-di-*tert*-butyl-2′-oxybenzyl)(2-pyridylmethyl)]amine}Cu(OAc) exhibited an irreversible one electron oxidation peaks at $E_{1/2}$ = 0.62 V (*vs.* Ag/AgCl) {CH_2Cl_2, TBAP, scan rate 100 mV s^{-1}}.[12] Apart from these structural analogues, another copper bisphenolate complex namely (*N*-benzyl-bis-*N*′,*N*″-salicylidene)-*cis*-1,3,5-triaminocyclohexanecopper(II) showed two reversible one-electron oxidations at $E_{1/2}$ = 0.89 V (0.34 V *vs.* Fc/Fc^+) and $E_{1/2}$ = 1.13 V (0.58 V *vs.* Fc/Fc^+) {0.1 mM in CH_2Cl_2, TBAB (500 mM), scan rate 200 mV s^{-1}}.[14c]

The electronic spectroscopy studies corroborated the electrochemical results. Specifically, the electronic spectra of the copper **1b** complex showed absorptions at 465 (ε = 823) and 673 nm (ε = 285 L mol^{-1} cm^{-1}) in addition to the ligand based π–π* transitions. The absorption at 465 nm is assigned to the equatorial phenolate–metal charge transfer (CT) band and is in agreement with similar absorption bands observed in the range of 370–460 nm for related complexes having an equatorial

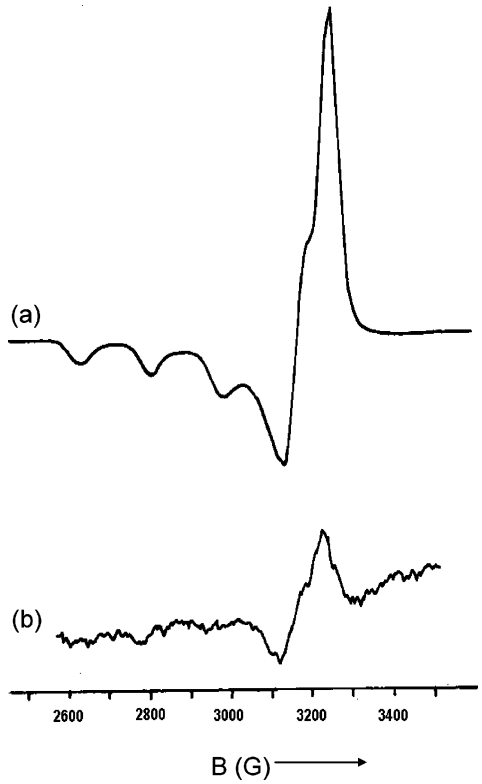

Fig. 4 X-Band EPR spectra of (a) the copper complex **1b** in CH_3CN at 77 K and (b) electrochemically generated cationic ^{1}**1b**$^+$ species in CH_3CN [TEAP (0.1 M)] at 77 K.

phenolate moiety bound to a Cu(II) center (Table S10 and Fig. S3, ESI†).[21,14n] The other absorption band appearing at 673 nm is assigned to a d–d transition and also falls in the range (640–780 nm) observed in analogous complexes.[14n] The *one-electron* oxidized species ^{1}**1b**$^+$ (as verified by EPR studies) generated electrochemically by exhaustive electrolysis carried out at +0.9 V, showed a red shift in the CT band at 465 nm (^{2}**1b**) to 500 nm (^{1}**1b**$^+$) and correlates with similar shift observed for a related analogue, namely {[(3-*tert*-butyl-5-methoxy-2-hydoxybenzyl)(3′-*tert*-butyl-5′-nitro-2′-oxobenzyl)(2-pyridylmethyl)]amine}Cu(OAc) (392 to 410 nm).[11]

The cyclic voltammetry results were substantiated by the density functional theory studies that ascribed the first *one-electron* oxidation to the loss of an electron from the equatorial phenolate-*O* moiety in ^{2}**1b** to give the lower energy ^{3}**1b**$^+$ while the second *one-electron* oxidation to that on the axial phenolic-*OH* moiety resulting in a dication ^{4}**1b**$^{2+}$ species. The three unpaired electrons of the dication ^{4}**1b**$^{2+}$ species reside on the Cu(II) $d_{x^2-y^2}$ orbital (150α), the equatorial phenolate-*O* moiety (149α) and the axial phenolic-*OH* moiety (148α) (Fig. 3). During the second *one-electron* oxidation process, the Mulliken net spin density on the Cu(II) (0.57) center and the equatorial phenolate (1.01) remains almost unchanged, while that on the axial phenolic-*OH* moiety drastically increases [0.02 (^{3}**1b**$^+$); 0.98 (^{4}**1b**$^{2+}$)] upon oxidation of ^{3}**1b**$^+$ to ^{4}**1b**$^{2+}$ species implying that the second oxidation is occurring on the axial phenolic-*OH* moiety (Table S9, ESI† and Fig. 3). In this context it is worth mentioning that unlike what is observed in the **1b** complex, where the two successive *one-electron* oxidations occur on the equatorial phenolate-*O* and the axial phenolic-*OH* moieties with the loss of net spin densities upon oxidation remaining confined to the respective phenyl moieties, theoretical calculations carried out on another related GOase model namely (*N*-benzyl-bis-*N*′,*N*″-salicylidene)-*cis*-1,3,5-triaminocyclohexanecopper(II)[22] showed that for both the first as well as the second *one-electron* oxidations, the net spin density due to the unpaired electron resulting from the oxidation gets delocalized over the two phenol rings instead and this is presumably due to the presence of a highly conjugated ligand backbone attached to two symmetrical phenolate-*O* moieties.

An important structural parameter often used in indicating the extent of distortion is given by the trigonal index that provides a measure of the degree of trigonality in a five-coordinated complex that may vary from a trigonal bipyramidal ($\tau = 1$) to square pyramidal ($\tau = 0$) geometry.[23] The trigonal index 'τ' is given by $\tau = (\beta - \alpha)/60$, where β is the larger of the two largest basal angles, α and β, in a five-coordinated geometry. Comparison of the optimized geometry of the neutral copper ^{2}**1b** complex with the *one-electron* oxidized species ^{3}**1b**$^+$ and the *two-electron* oxidized species ^{4}**1b**$^{2+}$ reveals that the *two-electron* oxidized species ^{4}**1b**$^{2+}$ species ($\tau = 0.57$) is significantly distorted from the *one-electron* oxidized ^{3}**1b**$^+$ species ($\tau = 0.11$) and the neutral copper ^{2}**1b** complex ($\tau = 0.21$). Indeed, a careful examination of the computed geometry optimized structure of ^{4}**1b**$^{2+}$ reveals that the axial phenolic-*OH* moiety, present in ^{2}**1b** and ^{3}**1b**$^+$, underwent deprotonation with a concomitant proton transfer to the metal bound acetate moiety (Fig. S4 and Table S8, ESI†). Further understanding of the proton transfer process occurring between the axial phenolic-*OH* and the metal bound acetate moieties were obtained from that the quasi-reversible cyclic voltammogram peak for oxidation of ^{1}**1b**$^+$ (verified by EPR studies) to ^{4}**1b**$^{2+}$ [$E_{1/2}$ = 1.10 V *vs.* Ag/AgCl] that exhibited a ΔE of 94 mV for the redox couple and is suggestive of a fast reversible proton transfer between the two on a CV timescale.

Significantly enough, the **1b** complex not only mimicked the active-site structure and the anti-ferromagnetic coupling present between the tyrosine (272) radical and the neighboring Cu(II) center in the active form of the GOase, but also successfully oxidized primary alcohols to aldehydes similar to the active enzyme. Specifically, when a variety of substituted benzylic alcohols were stirred under O_2 in presence of 0.1 mol% of the copper catalyst and 2 mol% of base (NaOH) at room temperature in CH_3CN, the corresponding aldehydes were obtained in moderate to high TONs (103–272) (Table 1). The broad substrate specificity of **1b** is underscored from its ability to successfully oxidize a wide range of substituted benzylic alcohol substrates to the corresponding aldehydes under ambient conditions. Quite remarkably, the **1b** complex reproduces the chemoselectivity of the enzyme GOase as it only oxidizes primary alcohols but fails in the case of secondary alcohols like cyclohexanol, for which no conversion to the ketone was observed even after 24 h. Worth noting that the efficiency of the **1b** complex is comparable to, and in many cases, even superior to that of other reported examples. For instance, a structurally similar functional GOase model namely, {[(3-*tert*-butyl-5-methoxy-2-hydoxybenzyl)(3′-*tert*-butyl-5′-nitro-2′-oxobenzyl)(2-pyridylmethyl)]amine}Cu(OAc) exhibited a maximum of 220 turnover numbers for the oxidation of benzyl alcohol in 48 h (KOH used as base, RT),[11] while the same was achieved by the **1b** complex in 24 h (272

Table 1 Selected results for the oxidation of primary alcohols by **1b**[a,b]

Entry	Reagent	Product	TON
1	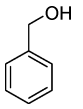	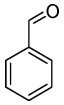	272
2	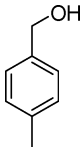	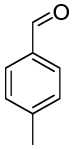	124
3	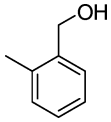	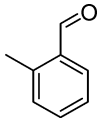	103
4	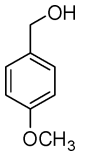	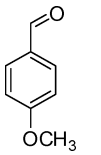	163
5	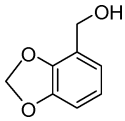	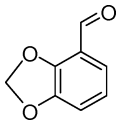	162
6	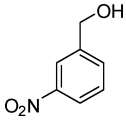	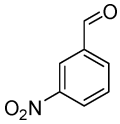	126
7	$CH_3(CH_2)_6OH$	$CH_3(CH_2)_5CHO$	10

[a] *Reaction conditions*: Benzylic alcohol, NaOH and 1,2-dichlorobenzene (internal standard) in the molar ratio of 1 : 0.02 : 1 in CH_3CN (10 mL), copper complex **1b** (0.001 mmol), 24 h at room temperature under O_2 atmosphere. [b] Determined by GC using 1,2-dichlorobenzene as an internal standard.

turnover numbers). Again, for the oxidation of benzyl alcohol to benzaldehyde, the activity of **1b** is also comparable to other functional models such as (*N*-benzyl-bis-*N*′,*N*″-salicylidene)-*cis*-1,3,5-triaminocyclohexanecopper(II) [44 turnover numbers in 24 h, 4% base, chemical oxidant ($Cu(CF_3SO_3)_2$ used, air, CH_3CN][14c] and [bis(di-*tert*-butylsalicylimine)binaphthyl]copper(II) [40 turnover numbers in 20 h, 0.2 mol% base, O_2, CH_3CN].[17] In this context it is worth mentioning that another copper complex, [*N*,*N*′-bis(2-oxy-3,5-di-*tert*-butylbenzyl)-1,2-ethylenediamine]copper(II), too showed similar broad substrate specificity like that of complex **1b** for a wide range of aliphatic primary alcohols [ROH, R = CH_3, C_2H_5, C_3H_7, C_4H_9] but exhibited much lower turnover numbers.[16] Apart from above-mentioned complexes, which serve as both structural and functional models of GOase, there are other complexes which though do not structurally mimic the active-site of GOase, but incorporates the other salient features of the GOase like the organic radical–Cu(II/I) redox couple and also successfully oxidizes primary alcohols to aldehydes under ambient aerobic conditions.[10a,b,15] For example, the copper complex [$CuL^{Se}(NEt_3)$] [where LH_2 = 2,2′-selenobis-(4,6-di-*tert*-butylphenol)] effectively carried out the oxidation of benzyl alcohol to benzaldehyde in up to 95 turnovers.[24]

It is worth noting that though the copper **1b** complex efficiently oxidizes a variety of substituted benzylic alcohols, similar to the other synthetic analogues, its activity is however, significantly lower compared to that of the active GOase enzyme. This difference in activity is ascribed to the better delocalization of the phenoxy radical into the equatorial tyrosine ring (Tyr 272) of the active enzyme[25] relative to that in the models, where structural constraints do not facilitate such substantial delocalization of the phenoxy radical and thereby account for much subdued activity in these synthetic mimics of GOase. Efficient delocalization of the phenoxy radical by the phenolate ring is a prerequisite for the subsequent rate determining H atom abstraction step (HAT).[26] Thus, the choice of suitable spacers and substituents on the phenolate rings in the model complexes becomes important as it plays a significant role in dictating the enzymatic activity. It is noteworthy that the activation barrier for the alcohol oxidation is estimated to reduce dramatically with the incorporation of electron withdrawing substituents on the equatorial phenolate moiety in small molecule synthetic GOase models.[27]

The dominating effect of electron withdrawing phenolate substituents on the enzymatic activity is very much evident in the existing GOase synthetic analogues. In particular, {[(3-*tert*-butyl-5-methoxy-2-hydoxybenzyl)(3′-*tert*-butyl-5′-nitro-2′-oxobenzyl)(2-pyridylmethyl)]amine}Cu(OAc),[11] which is an excellent structural and functional mimic of GOase, contains an electron-withdrawing nitro substituent on the *para*-position and a bulky *tert*-butyl moiety on the *ortho*-position of the equatorial phenolate ring while, {[(3,5-di-*tert*-butyl-2-hydoxybenzyl)(3′,5′-di-*tert*-butyl-2′-oxobenzyl)(2-pyridylmethyl)]amine}Cu(OAc),[12] which only serves as a structural model but do not exhibit any functional characteristics, contains relatively more electron donating *tert*-butyl group on the *para*-position with the *ortho*-substituent remaining the same. The increased electron density due to the combined inductive effects of the two *tert*-butyl groups significantly diminishes the ability of the phenolate ring to delocalize the phenoxy radical in the functionally inactive {[(3,5-di-*tert*-butyl-2-hydoxybenzyl)(3′,5′-di-*tert*-butyl-2′-oxobenzyl)(2-pyridylmethyl)]amine}Cu(OAc)[12] complex. Quite understandably, owing to the presence of less electron donating methyl substituent on the *para*-position of the phenolate ring, complex **1b** was found to exhibit much superior activity than the inactive *ortho*/*para* di-*tert*-butyl substituted {[(3,5-di-*tert*-butyl-2-hydoxybenzyl)(3′,5′-di-*tert*-butyl-2′-oxobenzyl)(2-pyridylmethyl)]amine}Cu(OAc) complex.[12]

Apart from its utility in the biomimetic chemistry of GOase, the *green* aspect of the catalysis by the copper complex **1b** is worth commenting upon, particularly with regard to its potential use in the development of green oxidation catalysts. As these functional mimics were able to carry out controlled oxidation of several benzylic alcohols to aldehydes at ambient conditions using molecular O_2 (air), they offer potential solution towards circumventing the hazards associated with the use of stoichiometric amounts of traditional inorganic oxidants and waste disposal.

The most important feature of the copper complex **1b** is that, it not only mimics the structural and functional characteristics of GOase but also precisely emulates the enzyme mode

of action through an unconventional organic radical cofactor-Cu(II/I) redox coupled pathway. In order to get further insight about the catalytic cycle of the **1b** model complex we decided to model the oxidation of a specific alcohol substrate *e.g.* of benzyl alcohol. The proposed intermediates in the oxidation pathway were computed at the B3LYP/LANL2DZ 6–31G(d) level of theory by geometry optimizing the structures obtained after employing suitable modifications to the initial structure based on the neutral **1b** complex and taking into consideration other metal bound moieties of the various intermediates in the catalytic cycle (Scheme 4).

As proposed in the first step of the catalytic cycle, the neutral inactive **1b** complex undergoes *one-electron* aerial oxidation to generate the catalytically active radical cationic species ^{3}**1b**$^+$, which further binds to the alkoxide anion ($PhCH_2O^-$ moiety) with the elimination of the metal bound acetate. The computed geometry optimized structure of the intermediate **1** closely resembled the precursor ^{3}**1b**$^+$ species both structurally and electronically (Fig. S5 and Table S11, ESI†). The step 2 involves a hydrogen atom abstraction by the equatorial phenolate-*O* radical moiety from the methylene hydrogens of the metal bound alkoxy group of the intermediate **1** species[26] and which in turn generates a metal bound ketyl radical anion[28] that undergoes fast single electron transfer (SET) to give the aldehyde with concomitant reduction of metal center [Cu(II) to Cu(I)] forming a diamagnetic intermediate **2** species (Fig. S6, ESI†).[29] The kinetic isotope studies carried out on the enzyme and its model complexes revealed that the hydrogen atom transfer (HAT) is the rate-determining step as confirmed by its very high range (~7–54) of k_H/k_D values.[15,26,29] On the other hand, the single electron transfer (SET) is reported to be a rapid process.[10a,b] As expected, the structure and the electronic properties of the diamagnetic intermediate **2** is significantly different from that of the paramagnetic intermediate **1** species. Particularly, the equatorial Cu–O and Cu–N bond lengths in the intermediate **2** are comparatively larger than that of the intermediate **1** (Table S11, ESI†). In step 3, a dioxygen molecule replaces the metal bound aldehyde and subsequently carries out a *two-electron* oxidation in which the Cu(I) center of the intermediate **2** is oxidized back to Cu(II) along with the oxidation of the equatorial phenolate-*O* moiety to generate a phenolate-*O* radical, thereby resulting in the intermediate **3** species bearing a metal bound hydroperoxide moiety.[26] The intermediate **3**, again being paramagnetic in nature, is significantly different from the diamagnetic intermediate **2** species (Fig, S7 and Table S11, ESI†). The last step in the proposed catalytic cycle involves proton transfer from the $PhCH_2OH$ to the metal bound hydroperoxide moiety with the elimination of H_2O_2 and generating back the intermediate **1** species.

Conclusion

In summary, the copper complex, {[(3-*tert*-butyl-5-methyl-2-hydoxybenzyl)(3′-*tert*-butyl-5′-methyl-2′-oxobenzyl)(2-pyridylmethyl)]amine}Cu(OAc) **1b** was found to be an excellent structural and functional mimic of the enzyme GOase. Specifically, the binding of the tyrosine (272 and 495) and the histidine (496 and 581) residues to the copper center in the GOase enzyme were emulated by the two phenolate-*O* atoms and the amine N and pyridine *N*, respectively. In addition, the copper **1b** complex efficiently catalyzed the chemoselective oxidation of primary alcohols to the corresponding aldehydes in high turnover numbers under ambient conditions and, more importantly, it did so by employing a organic radical cofactor–Cu(II/I) redox couple analogous to the active enzyme.

Experimental

General procedures

All manipulations were carried out using a combination of a glovebox and standard Schlenk techniques. Solvents were purified and degassed by standard procedures. 2-(Aminomethyl)pyridine and 2-(*tert*-butyl)-4-methylphenol were purchased from Sigma Aldrich, Germany and used without any further purification. ^{1}H and ^{13}C {^{1}H} NMR spectra were recorded on a Varian 400 MHz

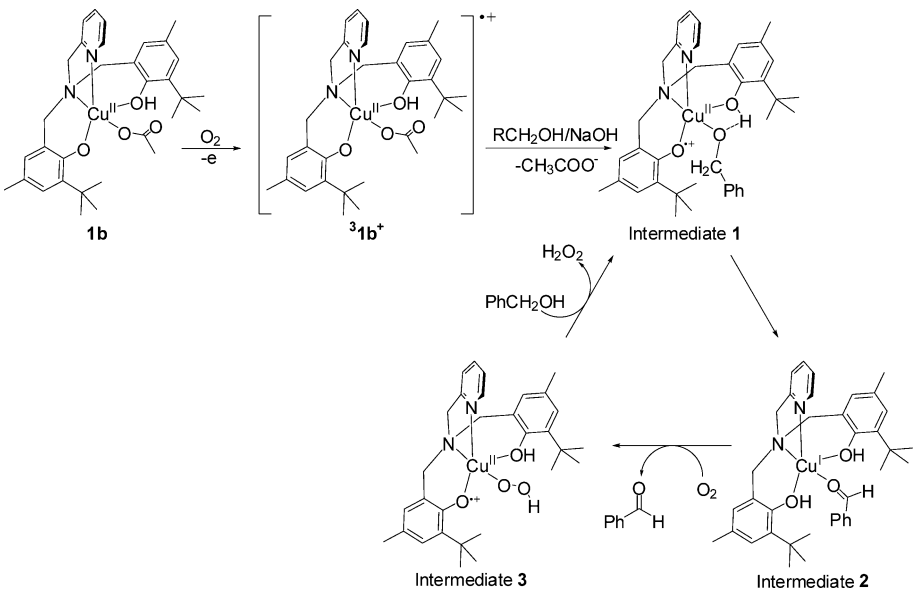

Scheme 4

NMR spectrometer. ^{1}H NMR peaks are labeled as singlet (s) and doublet (d). Infrared spectra were recorded on a Perkin Elmer Spectrum One FT-IR spectrometer. Mass spectrometry measurements were done on a Micromass Q-Tof spectrometer. The EPR measurements were made with a Varian model 109C E-line X-band spectrometer fitted with a quartz Dewar for measurements at 77 K. The spectra were calibrated by using tetracyanoethylene (tcne) ($g = 2.0037$). The electronic spectra were recorded in acetonitrile–dichloromethane (1 : 1) by using a Perkin Elmer Lambda 950 UV/VIS Spectrometer. GC spectra were measured on a Shimadzu gas chromatograph GC-15A equipped with a FID. Cyclic voltammetric and coulometric measurements were carried out using a PAR model 273A electrochemistry system. Platinum disc working (2 mm), auxiliary electrodes and Ag/AgCl electrode were used in three-electrode configuration. A platinum wire-gauze working electrode was used in coulometric experiments. Elemental Analysis was carried out on Thermo Quest FLASH 1112 SERIES (CHNS) Elemental Analyzer.

Synthesis of bis(3-*tert*-butyl-5-methyl-2-hydroxybenzyl)(2-pyridylmethyl)amine (1a)

2-Aminomethylpyridine (2.69 g, 24.9 mmol), 2-*tert*-butyl-4-methylphenol (8.19 g, 49.9 mmol) and formalin (8.42 g of 37% solution, 104 mmol) were taken in methnol (*ca.* 10 mL) and the reaction mixture was refluxed for 24 h during which time a precipitate was formed. The precipitate was isolated by filtration to obtain the product **1a** as a white powder (6.31 g, 55%). ^{1}H NMR ($CDCl_3$, 400 MHz, 25 °C): δ 10.2 (br, 2H, O*H*), 8.73 (d, 1H, $^3J_{HH} = 8$ Hz, *o*-C_5H_4N), 7.68 (t, 1H, $^3J_{HH} = 8$ Hz, *p*-C_5H_4N), 7.27 (t, 1H, $^3J_{HH} = 8$ Hz, *m*-C_5H_4N), 7.10 (d, 1H, $^3J_{HH} = 8$ Hz, *m*-C_5H_4N), 6.91 (s, 2H, *m*-C_6H_2), 6.66 (s, 2H, *m*-C_6H_2), 3.80 (s, 2H, CH_2), 3.72 (s, 4H, CH_2), 2.22 (s, 6H, CH_3), 1.36 (s, 18H, $C(CH_3)_3$). ^{13}C NMR ($CDCl_3$, 100 MHz, 25 °C): δ 156.0 (*ipso*-C_5H_4N), 153.8 (*o*-C_5H_4N), 148.1 (*ipso*-C_6H_2), 137.3 (*p*-C_5H_4N), 137.0 (*o*-C_6H_2), 128.9 (*p*-C_6H_2), 127.1 (*m*-C_6H_2), 127.0 (*m*-C_6H_2), 123.6 (*m*-C_5H_4N), 122.5 (*o*-C_6H_2), 122.0 (*m*-C_5H_4N), 56.1 (CH_2), 55.2 (CH_2), 34.7 ($C(CH_3)_3$), 29.5 ($C(CH_3)_3$), 20.7 (CH_3). LRMS (ES): m/z 461 $(M + H)^+$ 100%. HRMS (ES): calc. for $[M + H]^+$ 461.3168, found m/z 461.3156. IR (cm^{-1}, KBr pellet): 3048 (m), 2952 (s), 2865 (s), 2824 (m), 2370 (w), 1597 (m), 1478 (s), 1435 (s), 1375 (s), 1294 (m), 1236 (s), 1200 (s), 1151 (m), 1116 (m), 1010 (m), 933 (w), 859 (m), 752 (m), 682 (w), 630 (w). Anal. Calc. for $C_{30}H_{40}N_2O_2 \cdot CH_3OH$: C, 75.57; H, 9.00; N, 5.69. Found: C, 76.45; H, 9.55; N, 6.42%.

Synthesis of {[(3-*tert*-butyl-5-methyl-2-hydoxybenzyl)(3′-*tert*-butyl-5′-methyl-2′-oxobenzyl)(2-pyridylmethyl)]amine}Cu(OAc)} (1b)

To a stirred solution of $Cu(OAc)_2 \cdot H_2O$ (0.269 g, 1.35 mmol) in methanol (*ca.* 20 mL) was added a solution of bis(3-*tert*-butyl-5-methyl-2-hydroxybenzyl)(2-pyridylmethyl)amine (**1a**) (0.620 g, 1.35 mmol) in methanol (*ca.* 10 mL). The reaction mixture was refluxed for 8 h after which it was filtered and the filtrate was reduced under vacuum to obtain a dark solid. The residue was extracted with CH_3CN (*ca.* 10 mL) and filtered and the solvent was removed vacuum to obtain the product **1b** as a dark green solid (0.338 g, 43%). IR (cm^{-1}, KBr pellet): 3433 (w), 2958 (m), 2923 (m), 2855 (w), 1745 (w), 1683 (w), 1609 (m), 1597 (m), 1574 (s), 1467 (s), 1439 (s), 1414 (s), 1397 (s), 1290 (m), 1260 (m), 1229 (m), 1155 (w), 1122 (w), 1089 (w), 1069 (w), 1028 (m), 976 (w), 914 (w), 860 (m), 811 (w), 758 (w), 659 (m). Anal. Calc. for $C_{32}H_{42}CuN_2O_4 \cdot CH_3CN$: C, 65.52; H, 7.28; N, 6.74. Found: C, 64.90; H, 8.15; N, 7.58%.

Computational methods

Density functional theory calculations were performed on the copper **1b** complex (^{2}**1b**) and on its oxidized forms (^{3}**1b**$^+$ and ^{4}**1b**$^{2+}$) as well as on the mechanistic intermediates **1**, **2** and **3** using GAUSSIAN 03[30] suite of quantum chemical programs. The Becke three-parameter exchange functional in conjunction with Lee–Yang–Parr correlation functional (B3LYP) has been employed in the study.[31] The LANL2DZ basis set was used for Cu atom while the 6–31G(d) basis set was used for all other atoms. Stationary point calculations were carried out using the output coordinates from the geometry optimization calculations. Natural bond orbital (NBO) analysis was performed using the NBO 3.1 program implemented in the GAUSSIAN 03 package.[32]

General procedure for the aerobic oxidation of alcohols

In a typical catalysis run, a Schlenk flask was charged with the alcohol, NaOH and 1,2-dichlorobenzene (internal standard) in the molar ratio of 1 : 0.02 : 1 in CH_3CN (10 mL) and to this mixture was added the copper **1b** complex (0.001 mmol). The reaction mixture was stirred in an O_2 atmosphere for 24 h after which it was diluted with CH_3OH (10 mL) and analyzed by gas chromatography using 1,2-dichlorobenzene as an internal standard.

Crystallography

X-Ray diffraction data were collected on a Bruker P4 diffractometer equipped with a SMART CCD detector, and crystal data collection and refinement parameters are summarized in Table 2. The structures were solved using direct methods and standard

Table 2 X-Ray crystallographic data for **1b**

Formula	$C_{64}H_{84}Cu_2N_4O_8$
M_r	1164.43
Crystal system	Triclinic
Space group	$P\bar{1}$
a/Å	12.3083(4)
b/Å	14.719(2)
c/Å	18.0662(15)
α/°	73.601(10)
β/°	74.338(5)
γ/°	83.836(8)
V/Å^3	3021.6(5)
Z	2
T/K	120(2)
λ(Mo-Kα)/Å	0.71073
D_c/g cm^{-3}	1.280
μ(Mo-Kα)/mm^{-1}	0.760
θ_{max}/°	32.5654
No. of data	10584
No. of parameters	729
Reflections collected/unique	25774/10584
R_{int}	0.0294
R indices (all data)	$R1 = 0.0479$, $wR2 = 0.0853$
Final R indices [$I > 2\sigma(I)$]	$R1 = 0.0320$, $wR2 = 0.0768$
GOF	1.046

difference map techniques, and were refined by full-matrix least-squares procedures on F^2 with SHELXTL (Version 6.10).[33]

CCDC reference number 640145.

For crystallographic data in CIF or other electronic format see DOI: 10.1039/b801496e

Acknowledgements

We thank the Department of Science and Technology, New Delhi, for financial support of this research. We are grateful to the National Single Crystal X-ray Diffraction Facility at IIT Bombay for the crystallographic results. P. G. thanks Professor G. K. Lahiri and Professor A. Q. Contractor, IIT Bombay, for help with electrochemical studies. AJ thanks CSIR, New Delhi for research fellowship. Computational facilities from the IIT Bombay Computer Center are gratefully acknowledged.

References

1 (*a*) F. Thomas, *Eur. J. Inorg. Chem.*, 2007, 2379–2404; (*b*) J. W. Whittaker, *Chem. Rev.*, 2003, **103**, 2347–2363; (*c*) J. -L. Pierre, *Chem. Soc. Rev.*, 2000, **29**, 251–257; (*d*) E. I. Solomon, U. M. Sundaram and T. E. Machonkin, *Chem. Rev.*, 1996, **96**, 2563–2605; (*e*) J. P. Klinman, *Chem. Rev.*, 1996, **96**, 2541–2561.

2 (*a*) P. F. Knowles, R. D. Brown III, S. H. Koenig, S. Wang, R. A. Scott, M. A. McGuirl, D. E. Brown and D. M. Dooley, *Inorg. Chem.*, 1995, **34**, 3895–3902; (*b*) K. Clark, J. E. Penner-Hahn, M. Whittaker and J. W. Whittaker, *Biochemistry*, 1994, **33**, 12553–12557.

3 (*a*) N. Ito, S. E. V. Phillips, K. D. S. Yadav and P. F. Knowles, *J. Mol. Biol.*, 1994, **238**, 794–814; (*b*) N. Ito, S. E. V. Phillips, C. Stevens, Z. B. Ogel, M. J. McPherson, J. N. Keen, K. D. S. Yadav and P. F. Knowles, *Nature*, 1991, **350**, 87–90.

4 (*a*) A. Siebum, A. van Wijk, R. Schoevaart and T. Kieboom, *J. Mol. Catal. B: Enzym.*, 2006, **41**, 141–145; (*b*) D. Amaral, F. Kelly-Falcoz and B. L. Horecker, *Methods Enzymol.*, 1986, **9**, 87–92.

5 (*a*) J. W. Whittaker, *Arch. Biochem. Biophys.*, 2005, **433**, 227–239; (*b*) C. D. Borman, C. G. Saysell, A. Sokolowski, M. B. Twitchett, C. Wright and A. G. Sykes, *Coord. Chem. Rev.*, 1999, **190–192**, 771–779; (*c*) J. Stubbe and W. A. van der Donk, *Chem. Rev.*, 1998, **98**, 705–762.

6 (*a*) M. L. McGlashen, D. D. Eads, T. G. Spiro and J. W. Whittaker, *J. Phys. Chem.*, 1995, **99**, 4918–4922; (*b*) A. J. Baron, C. Stevens, C. Wilmot, K. D. Seneviratne, V. Blakeley, D. M. Dooley, S. E. V. Phillips, P. F. Knowles and M. J. McPherson, *J. Biol. Chem.*, 1994, **269**, 25095–25105; (*c*) B. P. Branchaud, M. P. Montague-Smith, D. J. Kosman and F. R. McLaren, *J. Am. Chem. Soc.*, 1993, **115**, 798–800; (*d*) G. T. Babcock, M. K. El-Deeb, P. O. Sandusky, M. M. Whittaker and J. W. Whittaker, *J. Am. Chem. Soc.*, 1992, **114**, 3727–3734; (*e*) M. M. Whittaker, V. L. DeVito, S. A. Asher and J. W. Whittaker, *J. Biol. Chem.*, 1989, **264**, 7104–7106.

7 (*a*) M. M. Whittaker and J. W. Whittaker, *J. Biol. Chem.*, 2003, **278**, 22090–22101; (*b*) M. S. Rogers and D. M. Dooley, *Curr. Opin. Chem. Biol.*, 2003, **7**, 189–196; (*c*) S. J. Firbank, M. S. Rogers, C. M. Wilmot, D. M. Dooley, M. A. Halcrow, P. F. Knowles, M. J. McPherson and S. E. V. Phillips, *Proc. Natl. Acad. Sci. U. S. A.*, 2001, **98**, 12932–12937.

8 M. M. Whittaker and J. W. Whittaker, *J. Biol. Chem.*, 1988, **263**, 6074–6080.

9 (*a*) F. Michel, F. Thomas, S. Hamman, C. Philouze, E. Siant-Aman and J.-L. Pierre, *Eur. J. Inorg. Chem.*, 2006, 3684–3696; (*b*) F. Michel, F. Thomas, S. Hamman, E. Siant-Aman, C. Bucher and J.-L. Pierre, *Chem.–Eur. J.*, 2004, **10**, 4115–4125; (*c*) A. Philibert, F. Thomas, C. Philouze, S. Hamman, E. Siant-Aman and J.-L. Pierre, *Chem.–Eur. J.*, 2003, **9**, 3803–3812.

10 (*a*) P. Chaudhuri, M. Hess, T. Weyehermüller and K. Wieghardt, *Angew. Chem., Int. Ed.*, 1999, **38**, 1095–1098; (*b*) P. Chaudhuri, M. Hess, U. Flörke and K. Wieghardt, *Angew. Chem., Int. Ed.*, 1998, **37**, 2217–2220; (*c*) M. Vaidyanathan, R. Viswanathan, M. Palaniandavar, T. Balasubramanian, P. Prabhaharan and T. P. Muthiah, *Inorg. Chem.*, 1998, **37**, 6418–6427; (*d*) A. Sokolowski, H. Leutbecher, T. Weyhermüller, R. Schnepf, E. Bothe, E. Bill, P. Hildebrandt and K. Wieghardt, *JBIC, J. Biol. Inorg. Chem.*, 1997, **2**, 444–453; (*e*) J. A. Halfen, B. A. Jazdzewski, S. Mahapatra, L. M. Berreau, E. C. Wilkinson, L. Que, Jr. and W. B. Tolman, *J. Am. Chem. Soc.*, 1997, **119**, 8217–8227; (*f*) S. Itoh, S. Takayama, R. Arakawa, A. Furuta, M. Komatsu, A. Ishida, S. Takamuku and S. Fukuzumi, *Inorg. Chem.*, 1997, **36**, 1407–1416; (*g*) D. Zurita, I. Gautier-Luneau, S. Ménage, J.-L. Pierre and E. Siant-Aman, *JBIC, J. Biol. Inorg. Chem.*, 1997, **2**, 46–55; (*h*) Y. Wang and T. D. P. Stack, *J. Am. Chem. Soc.*, 1996, **118**, 13097–13098.

11 F. Thomas, G. Gellon, I. Gautier-Luneau, E. Saint-Aman and J.-L. Pierre, *Angew. Chem., Int. Ed.*, 2002, **41**, 3047–3050.

12 Y. Shimazaki, S. Huth, A. Odani and O. Yamauchi, *Angew. Chem., Int. Ed.*, 2000, **39**, 1666–1669.

13 (*a*) P. Gamez, I. A. Koval and J. Reedijk, *Dalton Trans.*, 2004, 4079–4088; (*b*) S. Itoh, M. Taki and S. Fukuzumi, *Coord. Chem. Rev.*, 2000, **198**, 3–20; (*c*) B. A. Jazdzewski and W. B. Tolman, *Coord. Chem. Rev.*, 2000, **200–202**, 633–685.

14 (*a*) J. Xiang, Y.-G. Yin, P. Mei and Q. Li, *Inorg. Chem. Commun.*, 2007, **10**, 610–613; (*b*) F. Michel, S. Hamman, F. Thomas, C. Philouze, I. Gautier-Luneau and J.-L. Pierre, *Chem. Commun.*, 2006, 4122–4124; (*c*) A. K. Nairn, S. J. Archibald, R. Bhalla, B. C. Gilbert, E. J. MacLean, S. J. Teat and P. H. Walton, *Dalton Trans.*, 2006, 172–176; (*d*) A. dos Anjos, A. J. Bortoluzzi, R. E. H. M. B. Osório, R. A. Peralta, G. R. Friedermann, A. S. Mangrich and A. Neves, *Inorg. Chem. Commun.*, 2005, **8**, 249–253; (*e*) M. Taki, H. Hattori, T. Osako, S. Nagatomo, M. Shiro, T. Kitagawa and S. Itoh, *Inorg. Chim. Acta*, 2004, **357**, 3369–3381; (*f*) R. C. Pratt, L. M. Mirica and T. D. P. Stack, *Inorg. Chem.*, 2004, **43**, 8030–8039; (*g*) R. J. M. K. Gebbink, M. Watanabe, R. C. Pratt and T. D. P. Stack, *Chem. Commun.*, 2003, 630–631; (*h*) A. Neves, A. dos Anjos, A. J. Bortoluzzi, B. Szpoganicz, E. W. Schwingel and A. S. Mangrich, *Inorg. Chim. Acta*, 2003, **356**, 41–50; (*i*) R. J. Butcher, O. McKern and G. M. Mockler, *J. Chem. Crystallogr.*, 2003, **33**, 891–895; (*j*) M. Taki, H. Kumei, S. Nagatomo, T. Kitagawa, S. Itoh and S. Fukuzumi, *Inorg. Chim. Acta*, 2000, **300–302**, 622–632; (*k*) J. Müller, T. Weyhermüller, E. Bill, P. Hildebrandt, L. Ould-Moussa, T. Glaser and K. Wieghardt, *Angew. Chem., Int. Ed.*, 1998, **37**, 616–619; (*l*) S. Ito, S. Nishino, H. Itoh, S. Ohba and Y. Nishida, *Polyhedron*, 1998, **17**, 1637–1642; (*m*) H. Adams, N. A. Bailey, I. K. Campbell, D. E. Fenton and Q.-Y. He, *J. Chem. Soc., Dalton Trans.*, 1996, 2233–2237; (*n*) H. Adams, N. A. Bailey, C. O. Rodreguez de Barbarin, D. E. Fenton and Q.-Y. He, *J. Chem. Soc., Dalton Trans.*, 1995, 2323–2331.

15 P. Chaudhuri, M. Hess, J. Müller, K. Hildenbrand, E. Bill, T. Weyhermüller and K. Wieghradt, *J. Am. Chem. Soc.*, 1999, **121**, 9599–9610.

16 E. Saint-Aman, S. Ménage, J.-L. Pierre, E. Defrancq and G. Gellon, *New J. Chem.*, 1998, 393–394.

17 Y. Wang, J. L. DuBios, B. Hedman, K. O. Hodgson and T. D. P. Stack, *Science*, 1998, **279**, 537–540.

18 R. M. Wachter and B. P. Branchaud, *J. Am. Chem. Soc.*, 1996, **118**, 2782–2789.

19 R. D. Bereman and D. J. Kosman, *J. Am. Chem. Soc.*, 1977, **99**, 7322–7325.

20 (*a*) A. John, V. Katiyar, K. Pang, M. M. Shaikh, H. Nanavati and P. Ghosh, *Polyhedron*, 2007, **26**, 4033–4044; (*b*) N. Raman, V. Muthuraj, S. Ravichandran and A. Kulandaisamy, *Proc. Indian Acad. Sci. (Chem. Sci.)*, 2003, **115**, 161–167; (*c*) N. Raman, Y. P. Raja and A. Kulandaisamy, *Proc. Indian Acad. Sci. (Chem. Sci.)*, 2001, **113**, 183–189; (*d*) P. S. Subramanian, E. Suresh and D. Srinivas, *Inorg. Chem.*, 2000, **39**, 2053–2060; (*e*) B. J. Hathaway, *Struct. Bonding*, 1984, **57**, 55–118; (*f*) B. J. Hathaway and D. E. Billing, *Coord. Chem. Rev.*, 1970, **5**, 143–207.

21 (*a*) R. Uma, R. Viswanathan, M. Palaniandavar and M. Lakshminarayanan, *J. Chem. Soc., Dalton Trans.*, 1994, 1219–1226; (*b*) K. D. Karlin, B. I. Cohen, J. C. Hayes, A. Farooq and J. Zubieta, *Inorg. Chem.*, 1987, **26**, 147–153.

22 E. Zueva, P. H. Walton and J. E. McGrady, *Dalton Trans.*, 2006, 159–167.

23 A. W. Addison, T. N. Rao, J. Reedijk, J. van Rijn and G. C. Vershoor, *J. Chem. Soc., Dalton Trans.*, 1984, 1349–1356.

24 T. K. Paine, T. Weyhermüller, K. Wieghardt and P. Chaudhari, *Dalton Trans.*, 2004, 2092–2101.

25 U. Röthlisberger, P. Carloni, K. Doclo and M. Parrinello, *JBIC, J. Biol. Inorg. Chem.*, 2000, **5**, 236–250.

26 M. M. Whittaker, D. P. Ballou and J. W. Whittaker, *Biochemistry*, 1998, **37**, 8426–8436.

27 L. Guidoni, K. Spiegel, M. Zumstein and U. Röthlisberger, *Angew. Chem., Int. Ed.*, 2004, **43**, 3286–3289.

28 R. M. Wachter, M. P. Montague-Smith and B. P. Branchaud, *J. Am. Chem. Soc.*, 1997, **119**, 7743–7749.

29 M. M. Whittaker and J. W. Whittaker, *Biochemistry*, 2001, **40**, 7140–7148.

30 M. J. Frisch, G. W. Trucks, H. B. Schlegel, G. E. Scuseria, M. A. Robb, J. R. Cheeseman, J. A. Montgomery, Jr., T. Vreven, K. N. Kudin, J. C. Burant, J. M. Millam, S. S. Iyengar, J. Tomasi, V. Barone, B. Mennucci, M. Cossi, G. Scalmani, N. Rega, G. A. Petersson, H. Nakatsuji, M. Hada, M. Ehara, K. Toyota, R. Fukuda, J. Hasegawa, M. Ishida, T. Nakajima, Y. Honda, O. Kitao, H. Nakai, M. Klene, X. Li, J. E. Knox, H. P. Hratchian, J. B. Cross, V. Bakken, C. Adamo, J. Jaramillo, R. Gomperts, R. E. Stratmann, O. Yazyev, A. J. Austin, R. Cammi, C. Pomelli, J. Ochterski, P. Y. Ayala, K. Morokuma, G. A. Voth, P. Salvador, J. J. Dannenberg, V. G. Zakrzewski, S. Dapprich, A. D. Daniels, M. C. Strain, O. Farkas, D. K. Malick, A. D. Rabuck, K. Raghavachari, J. B. Foresman, J. V. Ortiz, Q. Cui, A. G. Baboul, S. Clifford, J. Cioslowski, B. B. Stefanov, G. Liu, A. Liashenko, P. Piskorz, I. Komaromi, R. L. Martin, D. J. Fox, T. Keith, M. A. Al-Laham, C. Y. Peng, A. Nanayakkara, M. Challacombe, P. M. W. Gill, B. G. Johnson, W. Chen, M. W. Wong, C. Gonzalez and J. A. Pople, *GAUSSIAN 03 (Revision C.02)*, Gaussian, Inc., Wallingford, CT, 2004.

31 (*a*) A. D. Becke, *Phys. Rev. A: At., Mol., Opt. Phys.*, 1988, **38**, 3098–3100; (*b*) C. Lee, W. Yang and R. G. Parr, *Phys. Rev. B: Condens. Matter Mater. Phys.*, 1988, **37**, 785–789.

32 A. E. Reed, L. A. Curtiss and F. Weinhold, *Chem. Rev.*, 1988, **88**, 899–926.

33 G. M. Sheldrick, *SHELXTL*, version 6.10, Bruker AXS, Inc., Madison, WI, 2000.

